

## Thermal and Morphological Properties of Thermoplastic Elastomer Nanocomposites Based on PA6/NBR

P. Mahallati<sup>1</sup>, A. Arefazar<sup>2\*</sup>, Gh. Naderi<sup>3</sup>

1- Higher Education Department, Islamic Azad University South Branch, Tehran, Iran.

2- Polymer Engineering Department, Amirkabir University of Technology, Tehran, Iran.

3- Iran Polymer & Petrochemical Institute (IPPI), Tehran, Iran

### Abstract

Morphological and thermal properties of PA6/NBR nanocomposites prepared through a direct melt mixing process in an internal mixer were studied. The effects of the NBR content (10, 30, and 50%) and nanoclay loading (3, 5, and 7%) on the microstructure properties of nanocomposites have been reported and compared with PA6/NBR blends as well. The thermoplastic elastomer (TPE) nanocomposites were characterized by X-ray diffraction (XRD), transmission electron microscopy (TEM), scanning electron microscopy (SEM), volume swelling in oil, differential scanning calorimeter (DSC) and dynamic mechanical thermal analysis (DMTA). XRD results show that Cloisite 30B is exfoliated into the PA6 and NBR. TEM image of the PA6/NBR/nanoclay composite confirms partial exfoliated structure of silicate layers dispersed into the both NBR and PA6 phases. The SEM photomicrograph of PA6/NBR nanocomposite shows an increasing of the rubber particles size in comparison with unfilled PA6/NBR TPE. By the presence of nanoclay, improved oil resistances of the prepared TPE nanocomposites were achieved. DSC studies show that loading of the nanoclay reduces the degree of crystallinity of the nanocomposite samples. The DMTA test shows that storage modulus of the PA6/NBR nanocomposite increases in comparison with the PA6/NBR blend. It also explains a reduction in damping by loading of the nanoclay.

**Keywords:** Nanocomposites, Thermoplastic Elastomers, Polyamide 6, NBR, Nanoclay

### 1- Introduction

Thermoplastics can simply be described as being able to deform plastically and flow on heating [1]. Polyamides, or nylons, thermoplastics have attracted interest in the past by virtue of their excellent strength properties, stiffness, chemical and wear resistances, low friction and high melting points [2]. Thermoplastic elastomers based

on polyamides, prepared by melt mixing with suitable rubbers like NBR are expected to have excellent hot oil resistance and high strength properties at elevated temperatures [3]. Several articles presenting studies on different properties of the PA6/NBR blends are available in the literature. Radhesh Kumar et al. have studied the effect of blend ratio, dynamic vulcanization, compati-

---

\* Corresponding author: Arefazar@aut.ac.ir

bilization and temperature on the flow behavior of the nylon/NBR thermoplastic elastomers [4]. Chowdhury et al. have reported improved strength and set properties of a carboxylated NBR/PA6/66/610 terpolymer composition [5]. Mehrabzadeh et al. have investigated the effect of different systems of curing and the amount of curing agent on thermal behavior and morphology of NBR/PA6 blends [6]. Although layered silicates such as clay are well-known filler materials, their interaction and exfoliation have attracted considerable attention as a route leading to the preparation of nanocomposites [7]. Moreover, many scientists are interested in polymer nanocomposites due to their unique properties comparative to pure polymers and typical composites. Naderi et al. have studied dynamically-vulcanized nanocomposite TPEs while investigating the effect of blend viscosity ratio and clay concentration on their microstructure and mechanical properties [8]. Kelnar et al. have focused on the compatibilizing ability of clay in dependence on elastomer structure and the dependence of mechanical properties on the resulting morphology [9]. Li et al. have identified the effect of clay addition on the morphology and thermal behavior of Polyamide 6 [10]. Furthermore, it has been suggested that stronger interactions between the clay particles and the Polyamide melt, result in better dispersion and exfoliation of clay platelets [11]. Our work presents experiments on the thermal and morphological properties of the PA6/NBR nanocomposites prepared through a direct melt mixing process. The effects of NBR and nanoclay contents on the microstructure and

thermal properties of the PA6/NBR TPE nanocomposites have been reported.

## 2- Experimental

### 2.1- Materials

The characteristics of the materials used in this work are given in Table 1. Polyamide 6 (PA6) Akulon F130-B was supplied by DSM Co. (Netherlands). Acrylonitrile Butadiene Rubber (NBR) Kosyn-KNB 35L was purchased from Kumho Petrochemical Co. (Korea) and the nanoclay used was Cloisite 30B, obtained from Southern Clay Products (USA), which is a natural montmorillonite modified with methyl, tallow, bis-2-hydroxyethyl, quaternary ammonium.

**Table 1.** Characteristics of the materials used.

Materials	Characteristics
PA6	Density (g/cc): 1.13 Melting Point (°C): 220
NBR	Density (g/cc): 0.94 Bound Acrylonitrile (%): 34 Mooney Viscosity, ML(1+4) at 100°C: 41
Nanoclay	Density (g/cc): 1.98 Modifier Concentration, meq/100g clay: 90 X-Ray Diffraction d-Spacing (Å): 18.5

### 2.2- TPE nanocomposite preparation

PA6 and nanoclay were dried at 80°C for 24 hr in a vacuum oven. The TPE nanocomposites based on PA6/ NBR/Cloisite 30B were prepared through a direct melt mixing process in a Haake Buchler Rheomix 750 internal mixer at 240°C and 80 rpm for 8 min. The samples formulations are given in Table 2. The compounds removed from the chamber were compression molded at 240°C

for 5 min to form 1-mm-thick sheets suitable for testing.

**Table 2.** The samples formulations (wt %).

Sample code	PA6 (wt %)	NBR (wt %)	Nanoclay (wt %)
PN10	90	10	0
PN30	70	30	0
PN50	50	50	0
PN10C3	87	10	3
PN30C3	67	30	3
PN50C3	47	50	3
PN10C5	85	10	5
PN30C5	65	30	5
PN50C5	45	50	5
PN10C7	83	10	7
PN30C7	63	30	7
PN50C7	43	50	7

### 2.3- Characterization

X-ray diffraction patterns (XRD) were obtained by using a Philips X'Pert (The Netherlands) at room temperature in the low angle of  $2\theta$  under a 50 kV voltage generator and a current of 40 mA. Transmission electron microscope (TEM) images of the TPE nanocomposites were obtained using a Philips CM-200 with an accelerator voltage of 200 kV. Phase structure was observed using a Philips XL30 scanning electron microscope. The cryogenically fractured samples were etched with toluene to extract the NBR phase, and sputter coated by a thin layer of gold before taking SEM micrographs. Volume swelling in the oil of the samples was measured by immersing the samples in the oil with an aniline point of  $77^\circ\text{C}$  for 70 hr at  $125^\circ\text{C}$  according to ASTM D-471 and the changes in weight were recorded. Crystallization behavior was

studied using a Maia-200F3 differential scanning calorimeter under nitrogen atmosphere. Samples were heated from 25 to  $260^\circ\text{C}$  at a rate of  $10^\circ\text{C}/\text{min}$  and then were cooled from 260 to  $25^\circ\text{C}$  after holding for 3 min and heated again from 25 to  $260^\circ\text{C}$  and held during 3 min at  $25^\circ\text{C}$ . Prior to DSC, the analysis samples were dried for 24 hr at  $100^\circ\text{C}$ . Dynamic mechanical thermal properties of the samples were carried out according to ASTM E1640-04 using a DMA, Tritec 2000, under the bending mode at a frequency of 1 Hz. The temperature range was from  $-100$  to  $100^\circ\text{C}$  and the specimens were heated at a rate of  $5^\circ\text{C}/\text{min}$ .

### 3- Results and discussion

#### 3.1- X-ray diffraction

The XRD results of TPE nanocomposites based on PA6/NBR with different nanoclay content and 10wt% of NBR are reported in Fig 1. Although the diffraction peak of Cloisite 30B appears at  $2\theta = 4.8^\circ$  [12], it can be seen that XRD peaks of the silicate layers have disappeared, indicating the exfoliation of the nanoclay into polymer matrix. As shown in Fig. 2, similar trends were observed for the XRD patterns of the PA6/NBR nanocomposites containing 3wt% nanoclay and different contents of the rubber (10, 30 and 50wt% NBR). Moreover, the decrease in the intensity of the XRD peaks with increasing NBR content is due to the increase in the viscosity and high shear stress, which also leads to the exfoliation of Cloisite 30B into the polymer matrix [8].

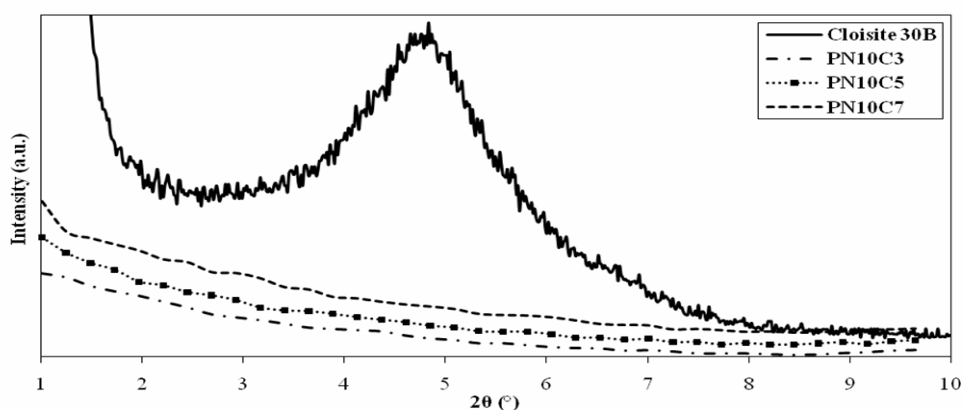


Figure 1. XRD patterns of Cloisite 30B, PN10C3, PN10C5 and PN10C7.

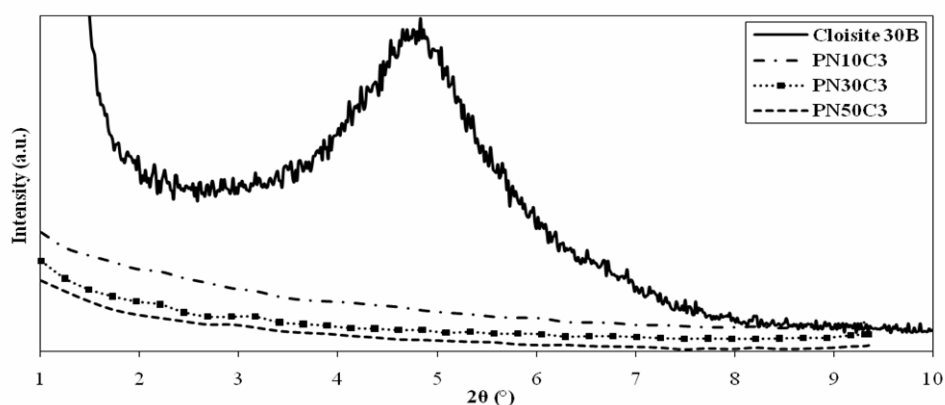


Figure 2. XRD patterns of Cloisite 30B, PN10C3, PN30C3 and PN50C3.

### 3.2- Transmission electron microscopy

The TEM image of PA6/NBR nanocomposite containing 30wt% NBR and 7wt% nanoclay is illustrated in Fig. 3. The rubber phase is white in color while the PA6 phase is darker. The nanoclay layers, dark lines in the TEM image, are dispersed throughout both the NBR and PA6 phases. It can be seen that a fraction of the silicate layers are exfoliated in the PA6 matrix, while a slight amount of the nanoclay remained in a clustered state. Therefore, the partially exfoliated structure of the silicate layers dispersed through PA6 matrix can be observed in this image.

### 3.3- SEM photomicrograph

A SEM image of the PA6/NBR (70/30) sample is shown in Fig. 4. The NBR phase, which has been etched by toluene can be seen as the dark holes dispersed throughout the PA6 phase. The average particle diameter size of the dispersed rubber phase is calculated by measuring the diameter size of about 50 randomly selected domains, which is about  $0.45 \pm 0.2 \mu\text{m}$ . A SEM image of the TPE nanocomposite based on PA6/NBR containing 30wt% NBR and 7wt% Cloisite 30B is shown in Fig. 5. As the average diameter particle size of rubber domains is measured (about  $1.06 \pm 0.4 \mu\text{m}$ ), it can be reported that the diameter size of rubber

particles has been increased by introduction of the nanoclay. The size of the dispersed rubber phase depends on the viscosity ratio and interfacial interactions between the NBR and the PA6 phases [8]. The presence of some nanoclay layers in the rubber phase

increases the viscosity ratio between the two phases, leading to an increase in the NBR particles size. TEM image also confirms the existence of some Cloisite 30B in the NBR phase.

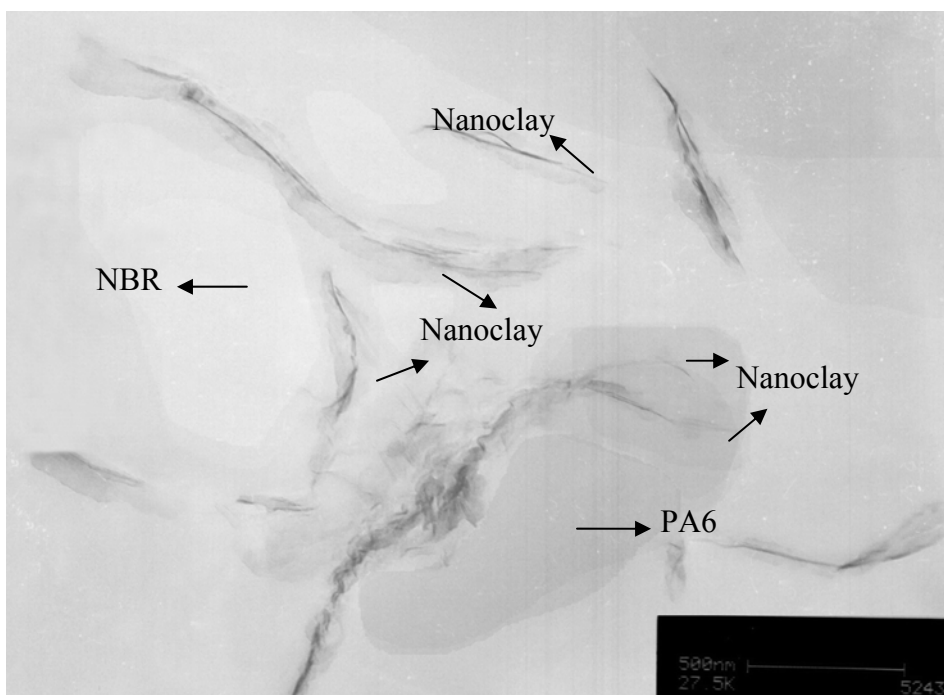


Figure 3. TEM micrograph of PN30C7

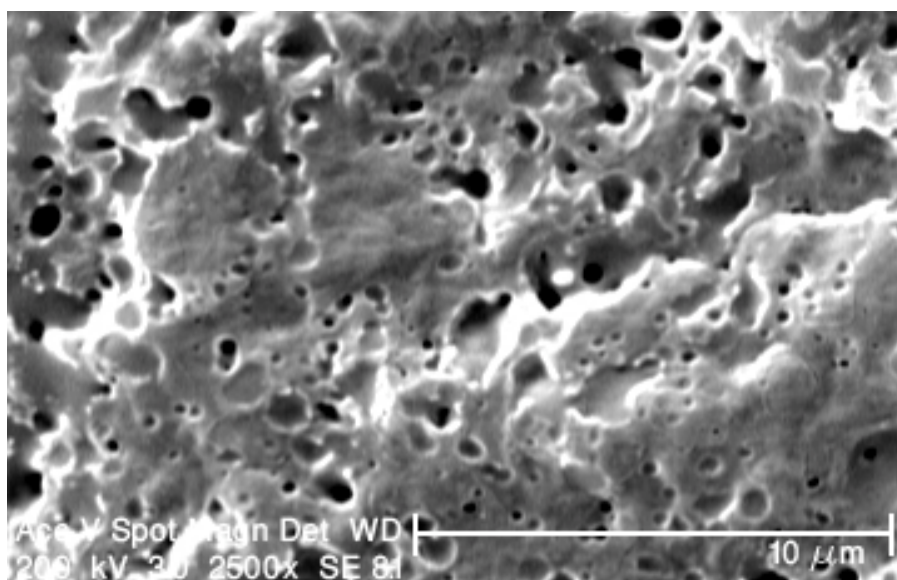
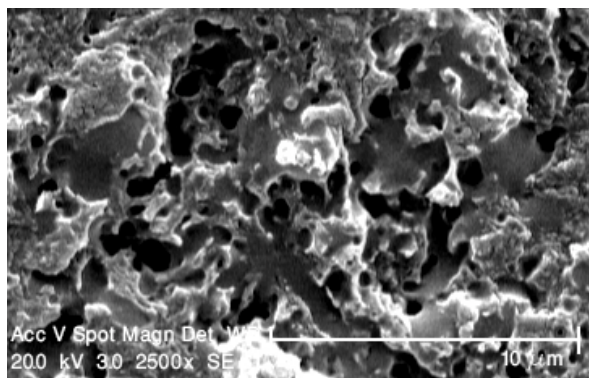


Figure 4. SEM photomicrograph of PA6/NBR (70/30)



**Figure 5.** SEM photomicrograph of PA6/NBR/nanoclay containing 30wt% NBR and 7wt% nanoclay.

### 3.4- Volume swelling in oil

Volume swelling for the samples was estimated as:  $q - 1 = [(W_2/W_1) - 1] \rho_c/\rho_s$ . Where  $q$  is the ratio of the swollen volume to the original unswollen volume, ( $q - 1 = \% \text{ of volume swell} / 100$ );  $W_1$  and  $W_2$  are specimen weights before and after swelling,

respectively;  $\rho_c$  and  $\rho_s$  are the density of the composition and the oil, respectively [13]. Fig. 6 shows a reduction in volume swelling in oil for nanocomposites of PA6/NBR=10, 30, 50wt% by the addition of the nanoclay content as well. It has been mentioned that the extent of swelling of a blend depends on the structure of the polymer phases and can be related to the properties of the polymer chains such as molecular mobility and phase interaction. As the nanoclay reinforces the polymer phase, its introduction should reduce the volume swell of the blend, and reduce the overall volume swelling of the nanocomposite in oil [14]. On the other hand, with the increased percentage of NBR, higher volume swellings in oil were observed. This is due to the lower swelling resistance of the rubber phase than PA6.

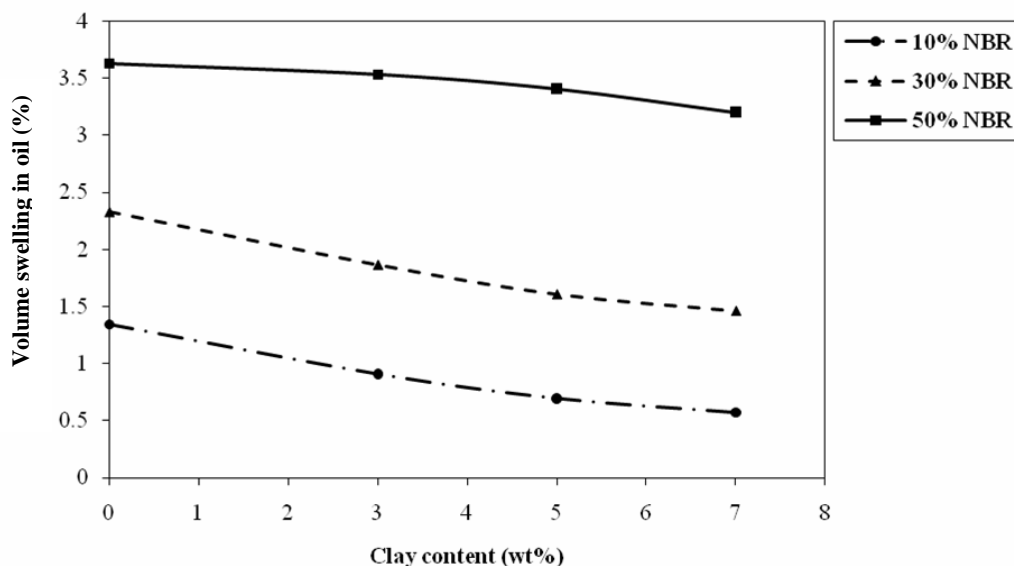


**Figure 6.** The effect of clay content on the volume swelling of PA6/NBR=10, 30, 50wt% nanocomposites.

### 3.5- DSC analysis

DSC thermograms of PA6/NBR (70/30) and PA6/NBR/nanoclay (63/30/7) samples are shown in Fig 7. The degree of crystallinity ( $\chi_c$ ), calculated by the ratio of  $\Delta H_m / \Delta H_m^\circ$ , decreases by adding 7% nanoclay as it is reported in Table 3.  $\Delta H_m^\circ$  is the heat of fusion of the purely crystalline forms of PA6, i.e. 240 J/g [15]. This decrease is due to the interaction between the nanoclay and the polymer matrix which reduces the crystallizable chain segments mobility [8, 15].

**Table 3.** Values of  $\Delta H_m$  and  $\chi_c$  of PN30 and PN30C7.

Sample	$\Delta H_m$ (J/g)	$\chi_c$ (%)
PN30	52.06	21.7
PN30C7	45.9	19.12

### 3.6- DMTA analysis

Figs. 8 and 9 show the storage modulus ( $E'$ ) and  $\tan \delta$  versus temperature for PA6/NBR (70/30) TPE and PA6/NBR nanocomposite containing 30wt% NBR and 7wt% nanoclay. As shown in Fig 8, the storage modulus of the PA6/NBR nanocomposite increases with nanoclay attendance, compared to PA6/NBR TPE. This increase in the storage modulus is because of strong interactions between the polymer matrix and the nanoclay interface [16]. The peak area under the  $\tan \delta$  curve at the glass transition is quantified by the energy dissipated during the dynamic experience and gives information about the viscous parts of the nanocomposites. As can be seen in Fig. 9, the  $\tan \delta$  peak area is reduced for the nanocomposite sample compared to the TPE based on PA6/NBR. This means that the damping is reduced by loading of the nanoclay [16].

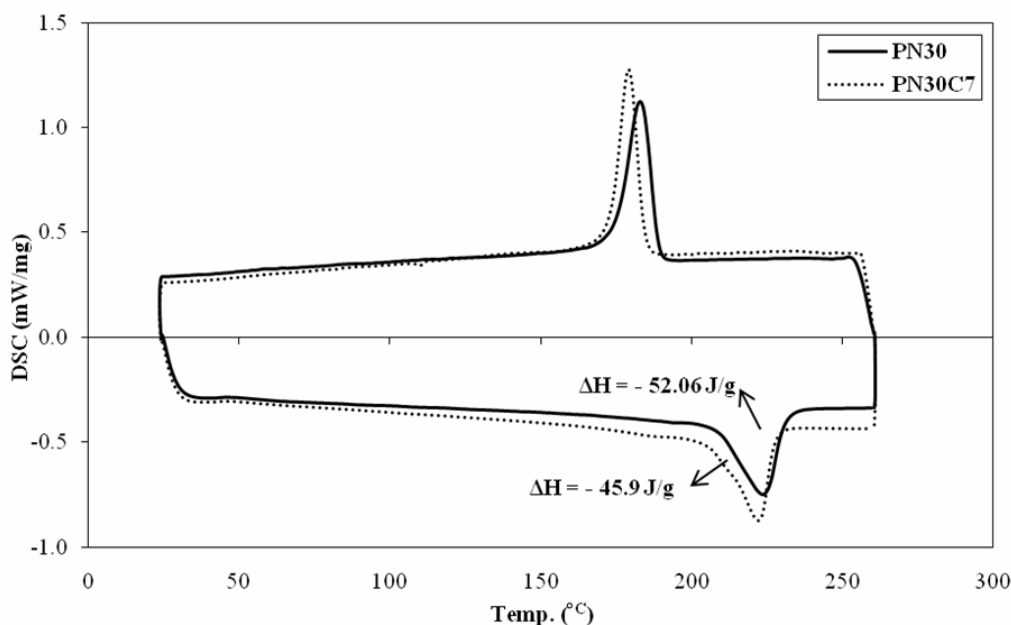


**Figure 7.** DSC thermograms of PN30 and PN30C7

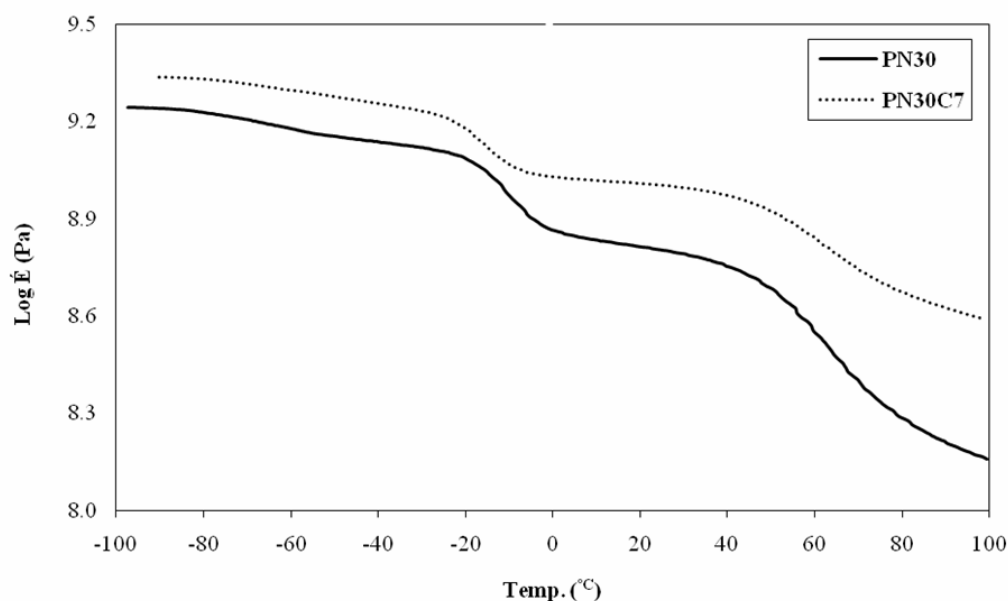


**Figure 8.** Storage modulus ( $E'$ ) versus temperature for PN30 and PN30C7.

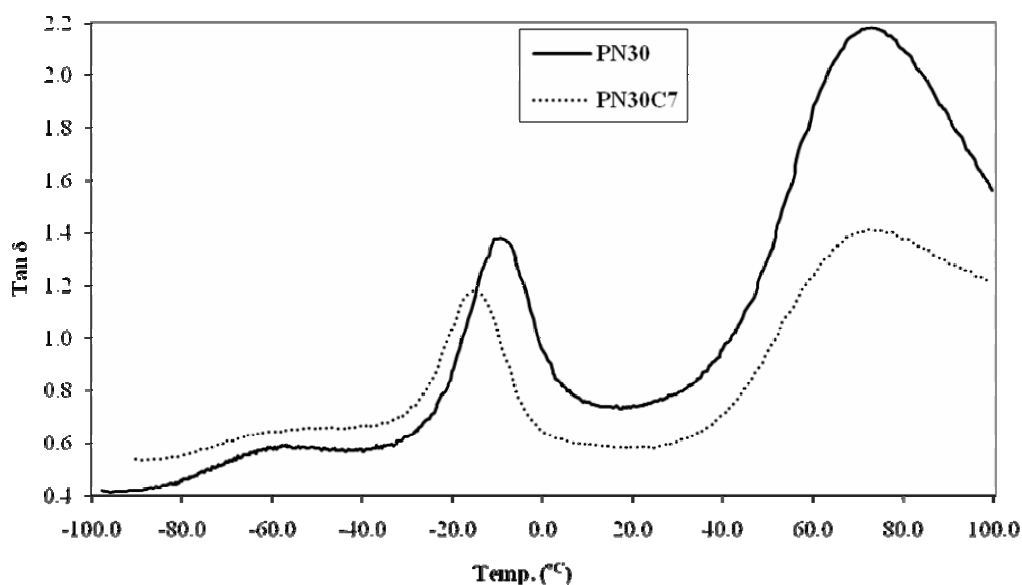


**Figure 9.**  $\tan \delta$  versus temperature for PN30 and PN30C7.

#### 4- Conclusions

We have prepared PA6/NBR nanocomposites containing 10, 30, 50wt% NBR and 3, 5, 7 wt% of the nanoclay by a direct melt mixing process. According to the

XRD, TEM and SEM results, Cloisite 30B was partially exfoliated into both the NBR and PA6 phases. DSC and DMTA studies indicated the strong interactions between the polymer matrix and the nanoclay interface in

TPE nano-composites based on PA6/NBR. The storage modulus of the PA6/NBR nanocomposites increased with nanoclay loading in comparison with that of the PA6/NBR blend. The  $\tan \delta$  of the nanocomposite sample was reduced in comparison with the unfilled PA6/NBR TPE. By introduction of nanosilicate layers into the PA6/NBR blend, the volume swelling of the nanocomposite was decreased.

## References

- [1] Bhattacharya Sati, N., Kamal Musa, R. and Gupta Rahul, K., Polymer nanocomposites theory and practice, Hanser publishers, p.341 (2008).
- [2] Wang, Z., Zhang, X., Zhang, Y., Zhang, Y. and Zhou, W., "Effect of dynamic vulcanization on properties and morphology of Nylon/SAN/NBR blends: A new compatibilization method of Nylon/ABS blends", Journal of Applied Polymer Science, 87 (13), 2057 (2003).
- [3] Coran, A.Y. and Patel, R., "Rubber-thermoplastic composites. Part II. NBR-Nylon thermo-plastic elastomer compositions", Rubber Chem. Technol., 53, 781 (1980).
- [4] Radhesh Kumar, C., Nair, V., George, K. E, Oommen, Z. and Sobu, T., "Blends of Nylon/Acrylonitrile Butadiene rubber: Effects of blend ratio, dynamic vulcanization and reactive compati-bilization on rheology and extrudate morphology", Polymer Engineering and Science, 43 (9), 1555 (2003).
- [5] Chowdhury, R., Banerji, M. S. and Shivakumar, K., "Polymer blends of Carboxylated Butadiene-Acrylonitrile copolymer (Nitrile rubber) and Polyamide 6 developed in twin screw extrusion", Journal of Applied Polymer Science, 104 (1), 372 (2007).
- [6] Mehrabzadeh, M. and Delfan, N., "Thermoplastic elastomers of Butadiene-Acrylonitrile copolymer and Polyamide. VI. dynamic crosslinking by different systems", Journal of Applied Polymer Science, 77 (9), 2057 (2000).
- [7] Kim, J-t. Oh, T-s. and Lee, D-h., "Morphology and rheological properties of nanocomposites based on nitrile rubber and organophilic layered silicates", Polymer Int., 52, 1203 (2003).
- [8] Naderi, G., Lafleur, P. G., Dubois, C., "Microstructure-properties correlations in dynamically vulcanized nano-composite thermoplastic elastomers based on PP/EPDM", Polymer Engineering and Science, 47 (3), 207 (2007).
- [9] Kelnar, I., Kotek, J., Kapralkova, L., Hromadkova, J. and Kratochvil, J., "Effect of elastomer type and functionality on the behavior of toughened polyamide nanocomposites", Journal of Applied Polymer Science, 100 (2), 1571 (2006).
- [10] Li, T-c., Ma, J., Wang, M., Tjiu, W. C., Liu, T. and Huang, W. "Effect of clay addition on the morphology and thermal behavior of Polyamide 6", Journal of Applied Polymer Science, 103 (2), 1191 (2007).
- [11] Borse, N.K. and Kamal, M.R., "Melt processing effects on the structure and mechanical properties of PA-6/Clay nanocomposites", Polymer Engineering and Science, 46 (8), 1094 (2006).
- [12] Perez, C. J., Alvarez, V. A., Mondragon, I. and Vazquez, A., "Mechanical properties of layered silicate/starch polycaprolactone blend nanocomposites", Polym. Int., 56 (5), 686 (2007).
- [13] Coran, A.Y., Patel, R. and Williams, D., "Rubber-thermoplastic compositios. Part VI. The swelling of vulcanized rubber-plastic compositions in fluids", Rubber Chem. Technol., 55, 1063 (1982).

- [14] Jha, A., Dutta, B. and Bhowmick, A.K., "Effect of fillers and plasticizers on the performance of novel heat and oil-resistant thermoplastic elastomers from Nylon-6 and Acrylate rubber blends", *Journal of Applied Polymer Science*, 74 (6), 1490 (1999).
- [15] Fornes, T.D. and Paul, D.R., "Crystallization behavior of Nylon 6 nanocomposites", *Polymer*, 44 (14), 3945 (2003).
- [16] Kim, J-t., Oh, T-s. and Lee, D-h., "Preparation and characteristics of nitrile rubber (NBR) nanocomposites based on organophilic layered clay", *Polym. Int*, 52 (7), 1058 (2003).